Particle Accelerators
1975, Vol. 6, pp. 201–209

SHUNT IMPEDANCE OF SPIRAL LOADED RESONANT RF CAVITIES†

PEYTON Z. PEEBLES, Jr. and M. PARVARANDEH

The University of Tennessee, Knoxville, Tennessee, U.S.A

and

C. M. JONES

Oak Ridge National Laboratory, Oak Ridge, Tennessee, U.S.A.

(*Received November 4, 1974*)

Based upon a treatment of the spiral loaded resonant radio frequency cavity as a shorted quarter-wave transmission line, a model for shunt impedance is developed. The model is applicable to loosely wound spirals in large diameter containers. Theoretical shunt impedance is given for spirals wound from tubing of circular or rectangular cross section. The former produces higher shunt impedance. Measurements made at Oak Ridge National Laboratory on 17 copper cavities are described which support the theoretical results. Theoretical results are also compared to data from twenty-three additional cavities measured at Los Alamos Scientific Laboratory. It is shown that the theoretical function forms a useful means of interpreting the quality of constructed cavities.

INTRODUCTION

Shunt impedance is one of the important parameters to be considered in the design of resonant radio frequency (rf) cavities for room-temperature linear accelerators. Achievable shunt impedance determines the required rf exciter power, which in turn, is a significant factor in cost. Thus, to help minimize cost one seeks an accelerating structure with large shunt impedance.

A resonant rf structure, in which there has been considerable recent interest for linear accelerators is the spiral loaded cavity (SLC) described by Dick and Shephard.[1] Early indications, based upon measurements,[1] are that the SLC can give a larger shunt impedance than the helix loaded cavity (HLC). This is an important result since the HLC has been a possible candidate structure for some variable-velocity profile heavy ion accelerators. It is all the more important when the structural superiority of the SLC as compared to the HLC is considered. The SLC is much less subject to vibrational instability than the HLC.

In this paper a model is developed to describe the shunt impedance of the SLC. The model is based upon a treatment of the SLC as a shorted quarter-wave transmission line and is strictly applicable only to loosely wound (large-radius) spirals housed in large containers. It is known that some SLC's give shunt impedances which exceed those predicted by the model. For such cases the model results serve to separate "good" from "poor" SLC's.

After a brief tutorial discussion of shunt impedance definitions, the model is developed for spirals wound from tubing having either circular or rectangular cross section, the former giving the best results. The resulting shunt impedance formulas are useful in inferring the optimum structure parameters. The theoretical results have been verified by measurements on 17 copper cavities at Oak Ridge National Laboratory. In addition, measurements on twenty-three cavities reported in reference 2 are compared with the theory and some inferences are drawn relative to the design of SLC's for maximum shunt impedance.

† Work reported was sponsored by the U.S. Atomic Energy Commission under contract with Union Carbide Corporation.

SHUNT IMPEDANCE OF RESONANT STRUCTURES

Two principal definitions are used for the shunt impedance of resonant structures.[3†] "Bare" shunt impedance Z is defined by

$$Z = \frac{[\int_0^L |E(z)|\,dz]^2}{PL}, \tag{1}$$

where $E(z)$ is the complex amplitude of the electric field on the accelerating axis z and P is the total average power dissipated in the structure of total length‡ L along the accelerating axis.

Although bare shunt impedance is most often used in comparing structures, "effective" shunt impedance Z_{eff} provides a more realistic relationship between acceleration capability and power loss. In the idealized case where the accelerated particle passes through the structure with constant velocity[3]

$$Z_{\text{eff}} = \rho^2 Z, \tag{2}$$

where, for the single-spiral SLC (special case of $n = 1$),

$$\rho = \frac{|\int_0^L E(z)e^{j2\pi z/L}\,dz|}{\int_0^L |E(z)|\,dz}. \tag{3}$$

The parameter ρ is the transit time factor when the field has a phase shift through the structure which is a multiple of π. Effective shunt impedance is never larger than bare shunt impedance since $\rho \leq 1.0$. Effective shunt impedance is more difficult to determine than bare shunt impedance because of the need to solve Eq. (3).

In this paper only bare shunt impedance is considered for the theoretical calculations since it is the most easily obtainable of the two, involves only structure parameters and is independent of particle velocity. However, since $|E(z)|$ must be determined in the course of measuring the 17 cavities mentioned above, ρ^2 was also found for these cavities. One may then obtain effective shunt impedance easily through use of (2).

† Due to common usage we use the term shunt impedance rather than the more correct statement shunt impedance per unit length. The unit of shunt impedance is ohms per unit length.

‡ Structure length is n wavelengths ($n = 1, 2, \ldots$) at the particle velocity v. Thus, $L = nv/f = n\beta\lambda$, where f is the operating frequency having free-space wavelength λ and β is particle relative phase velocity ($\beta = v/c$, c = speed of light). For the SLC with one spiral $n = 1$.

SLC MODEL

With respect to resonant frequency, the SLC behaves approximately as a shorted quarter-wave transmission line. Furthermore, the current along the spiral is known to have a magnitude similar to that of a quarter-wave line.[4] Using these facts we postulate that shunt impedance may also be determined by modeling the SLC as an appropriate quarter-wavelength shorted transmission line. The open end of the line then represents the SLC in the region of the accelerating axis.

To more firmly fix these points we describe a conceptual evolution of the SLC from a quarter-wave line as illustrated in Figure 1. We begin

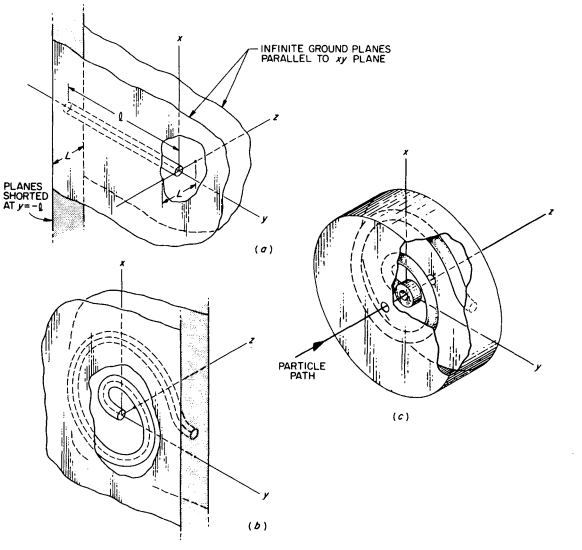

FIGURE 1 Conceptual evolution of a spiral loaded cavity. (a) A quarter wavelength transmission line, (b) the line after forming a spiral and (c) the spiral loaded cavity after distorting infinite ground planes.

with a uniform line having a center conductor mid-way between two infinite ground planes as shown in (a). The planes are connected at a distance $l = \lambda/4$ to create the quarter-wave line. If Z_o is the characteristic impedance of the unterminated line and α is the line attenuation coefficient (nepers per unit length), it is easily shown that the input impedance Z_i is approximately

$$Z_i = \frac{Z_o}{\alpha l} \tag{4}$$

if the line has small loss per unit length.

Next, suppose the center conductor is wound around itself as shown in Figure 1(b). If the turns are sufficiently separated and have sufficiently large radii the value of Z_i will be only slightly changed over that of a straight line. Finally, the infinite ground planes may be made finite and the conductor connecting these planes may be distorted into a circular shape and closed upon itself. The result of all these operations is still a quarter-wave line, however, it is now one contained in a reasonable enclosure for use as an accelerator structure. By cutting one hole in each of the two parallel planes at the z axis, and providing a hole at the end of the center conductor, as shown in (c), a particle path is placed in the region of maximum electric field.

We note that the model, as evolved, applies only to loosely wound spirals with turns having large radii and that the spiral container must not be too close to the outer spiral turn. Measurements taken to date indicate that "gaps" between the various conductor surfaces of about three or more times the largest cross-sectional dimension of the spiral are adequate to insure reasonable agreement between the model's theoretical shunt impedance and measured values.

The model becomes complete once the shunt impedance Z of the actual structure is related to the input impedance Z_i of the model equivalent line. The relationship is established by equating the average powers dissipated in the two structures. The power lost in the model line is

$$P = V^2/2Z_i, \tag{5}$$

where V is the peak potential difference between the center conductor and the outer cavity walls. We find V by integrating the peak electric field along the z axis

$$V = \frac{1}{2}\int_0^L |E(z)|\,dz. \tag{6}$$

Squaring (6) and substituting into (5) along with (4) gives the model line power loss. Equating this loss to P as found from (1) allows us to solve for Z:

$$Z = \frac{8Z_O}{\alpha l L}. \tag{7}$$

Our basic result (7) shows that bare shunt impedance does not depend on the field distribution along the axis; it is only a characteristic of the structure.

BARE SHUNT IMPEDANCE OF SLC MODEL

To obtain numerical results for the model developed in the last section the transmission line parameters Z_O and α must be determined. At this point it becomes necessary to specify a cross-section geometry for the spiral conductor. We carry out two developments based upon circular and rectangular cross sections.

Spirals Having Circular Cross-Section

Assume the spiral is wound from a tube having a diameter d_0. The characteristic impedance of the line is (Ref. 5):

$$Z_O = \frac{60}{\sqrt{\varepsilon_r}} \ln\left[\frac{4L}{\pi d_0}\right], \qquad d_0/L < 0.75, \tag{8}$$

where ε_r is the dielectric constant of the space between conductors.

To evaluate α we neglect losses in the dielectric in relation to conductor losses. Assuming all conductors to be of the same material we apply a method of Wheeler[6] as developed by Cohn.[7] The procedure leads to

$$\alpha = \frac{R_s}{2\pi Z_O L}\left(1 + \frac{L}{d_0}\right). \tag{9}$$

Here R_s is conductor surface resistance (ohms per square). For copper

$$R_s = 2.61(10^{-7})\sqrt{f} \tag{10}$$

with f being frequency in hertz.

Substitution of (8) and (9) allows (7) to be written as

$$\frac{R_s l \varepsilon_r Z}{3600\pi^3} = \frac{16\left[\ln\left(\frac{4L}{\pi d_0}\right)\right]^2}{\pi^2\left(1 + \frac{L}{d_0}\right)}, \quad 1.33 \le L/d_0, \tag{11}$$

for spirals with circular cross section. The right side of (11) may be considered as a normalized shunt impedance; it is plotted in Figure 2. By recognizing that $l = \lambda/4$ and $\lambda = c/f$, the dependence on l can be eliminated to obtain the same normalized shunt impedance, now equal to

$$R_s c \varepsilon_r Z/14{,}400\pi^3 f;$$

this form is also shown on Figure 2.

The value of L/d_0 giving the maximum in Figure 2 is 7.57. At the maximum for a copper

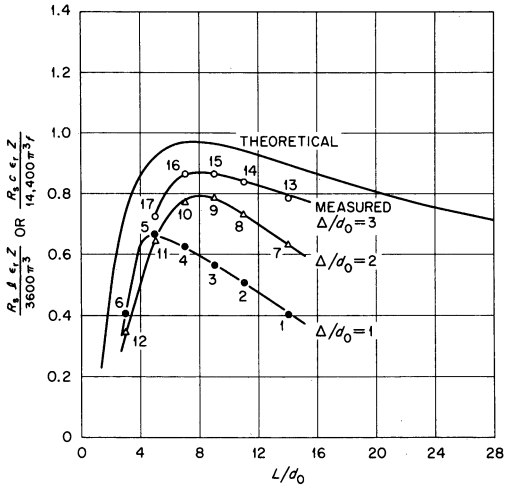

FIGURE 2 Theoretical and measured bare shunt impedance for spiral loaded cavities with spirals having circular cross section.

cavity $Z = 5560\sqrt{f}$ Ω/m. Thus, for example at 100 MHz, a bare shunt impedance of 55.6 MΩ/m can be achieved.

Spirals Having Rectangular Cross Section

For rectangular cross sections, Cohn[7] has given the characteristic impedance applicable to the model line:

$$Z_0 = \frac{60}{\sqrt{\varepsilon_r}} \ln\left[\frac{4L}{\pi d_0}\right], \frac{w}{L-t} \leq 0.35 \quad \text{and} \quad \frac{t}{L} \leq 0.25. \tag{12}$$

Here t is the spiral thickness in the axial or z direction, w is the width in the radial direction, and d_0 is the diameter of a circular conductor which is *equivalent* to the actual rectangular conductor. Equation (12) is thought to be accurate within 1.24% over the specified parameter range.[7]

A curve of d_0 as a function of w and t is given by Cohn.[7] However, the exact expression for the curve is too complex for practical use and the approach taken here is to use approximate results as follows:

$$\frac{d_0}{w} = 0.524 + 0.7475(t/w) - 0.0915(t/w)^2, \; t/w \leq 1.0 \tag{13}$$

$$\frac{d_0}{t} = 0.524 + 0.7475(w/t) - 0.0915(w/t)^2, \; w/t \leq 1.0. \tag{14}$$

Equation (13) is accurate to within about 0.5% of Cohn's curve for $0.1 \leq t/w \leq 1.0$ and to within about 5% for $0 \leq t/w \leq 0.1$. Similar comments apply to (14) for the parameter w/t.

In order to calculate shunt impedance α must first be found. It can be shown[7] that

$$\alpha = \frac{R_s}{2\pi Z_0 L}\left[1 + \frac{L}{d_0}\left(\frac{\partial d_0}{\partial w} + \frac{\partial d_0}{\partial t}\right)\right], \tag{15}$$

where Z_0 is given by (12). The term $\partial d_0/\partial w + \partial d_0/\partial t$ is again a function which must be approximated if one seeks closed-form results. The approximations

$$\frac{\partial d_0}{\partial w} + \frac{\partial d_0}{\partial t} = 1.154 + \frac{0.0207}{t/w}, \; t/w \leq 1.0 \tag{16}$$

$$= 1.154 + \frac{0.0207}{w/t}, \; w/t \leq 1.0 \tag{17}$$

are within 1% of Cohn's curve for $0.14 < t/w$ (or w/t) ≤ 1.0, and about 8% for $0.06 \leq t/w$ (or w/t) ≤ 0.14. The error rises rapidly for values below 0.06. Fortunately, one is usually not interested in data in the range less than 0.06.

Using (15) and (12) with (7) the bare shunt impedance becomes

$$\frac{R_s l \varepsilon_r Z}{\pi^3 (60)^2} = \frac{16 \ln^2\left[\frac{4L}{\pi d_0}\right]}{\pi^2\left[1 + \frac{L}{d_0}\left(\frac{\partial d_0}{\partial w} + \frac{\partial d_0}{\partial t}\right)\right]} \tag{18}$$

for $w/(L-t) \leq 0.35$, $t/L \leq 0.25$ and $0.14 < (t/w$ or $w/t)$ with an accuracy of a few percent. Figure 3 shows various plots of (18) where (13) and (16) were used for $t/w \leq 1.0$ and (14) and (17) apply when $t/w > 1.0$.

Several points are clear from Figure 3. First, an optimum value of L/t exists for every choice of t/w. The peak is a broad one, however, and the optimum value of Z does not change greatly for a large range of t/w values. Finally, the largest value of Z occurs for t/w of 1.0 and for L/t of 8.64. These points are illustrated in Figure 4 where the various optimum values are given as a function of t/w.

By comparing the $t/w = 1.0$ curve of Figure 3. with Figure 2 it is seen that higher shunt impedance (by a factor of 1.15) is realized with circular cross section spirals.

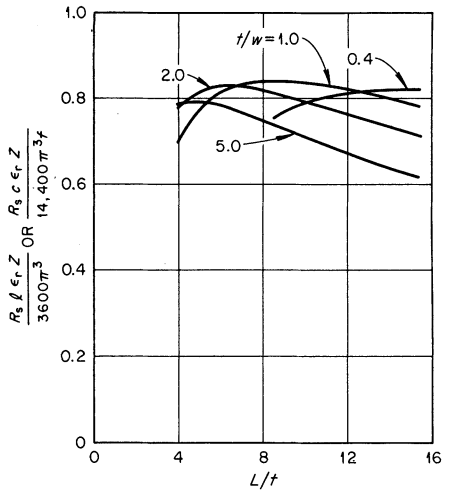

FIGURE 3 Theoretical bare shunt impedance for spiral loaded cavities with spirals having rectangular cross section.

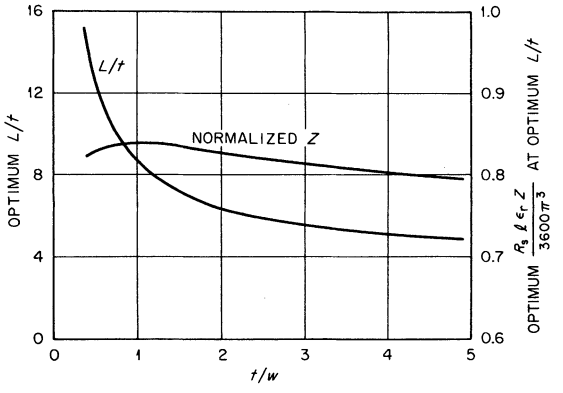

FIGURE 4 Optimum cavity length to spiral thickness ratio (L/t) and optimum bare shunt impedance for cavities with spirals of rectangular cross section. Here t/w is the spiral thickness to width ratio.

EXPERIMENTAL DATA

In order to verify the theoretical curve of Figure 2 three sets of measurements were made. Each measurement set corresponded to a sequence of shell lengths L obtained by progressively cutting down the length of one of three "initial" cavities. Of course only one "initial" cavity with L progressively reduced would have been sufficient to verify the behavior of Figure 2. However, it was decided to attempt also to illustrate that Figure 2 applies best to loosely wound spirals by performing three sets of measurements, one for each of three spiral gap spacings. Thus, the three "initial" cavities differed primarily in gap spacing.

Certain design parameters were identical for all three "initial" cavities. The drift tube was a thick-walled cylinder having an inside diameter D_D = 1.59 cm, outside diameter of 3.18 cm, and length along the accelerating axis of L_D = 1.27 cm. The spirals were all wound with N = 1.5 turns from round copper tubing having a diameter d_0 = 1.27 cm. The spirals were comprised of full semi-circular segments and portions of semi-circles originating from offset centers such that any adjacent turn segments were separated by a constant spiral gap distance. In other words, each spiral was wound to the same "law" which produced constant turns separation. Finally, all "initial" cavity shell lengths L were 17.78 cm.

The difference between the three "initial" cavities was gap spacing Δ. The three values selected were 1.27 cm, 2.54 cm, and 3.81 cm (d_0, $2d_0$, and $3d_0$). It was felt that $\Delta = 3d_0$ would give results near the theoretical values for loosely wound spirals while $\Delta = d_0$ would correspond more to a tightly wound spiral. Having set Δ, the stem lengths A (defined as the distance between shell inside surface at the spiral junction point and the outside surface of the spiral outer turn at the same point measured as though the spiral continued rather than turning into the outer wall) were also chosen to be d_0, $2d_0$, and $3d_0$. The choices Δ and A set the shell diameter D and spiral nominal length l. These values were: D = 17.9 cm, 26.5 cm, and 34.9 cm; l = 52.0 cm, 72.8 cm, and 92.0 cm. The three values of l correspond to design frequencies of 144.2 MHz, 103.0 MHz, and 81.5 MHz respectively.

The physical construction of a typical cavity is illustrated in Figure 5. This figure shows a medium diameter cavity (D = 26.5 cm) after L was reduced to 6.35 cm (5.0 d_0). All surfaces were machined or formed from solid copper. The joint where drift tube and spiral meet was soft-soldered and copper-plated. The junction of the spiral and shell was made tight by using an expanding plug within the hollow spiral tubing. The ends of the shell were cut with a 5 degree bevel to raise the inside edge and give a "knife-edge" joint with the end plates.

The three "initial" cavities were progressively reduced in shell length L and important performance parameters such as resonant frequency f_0, unloaded Q, Q_0, and bare shunt impedance Z were measured at each length. Table I summarizes measured results. Shunt impedance was found

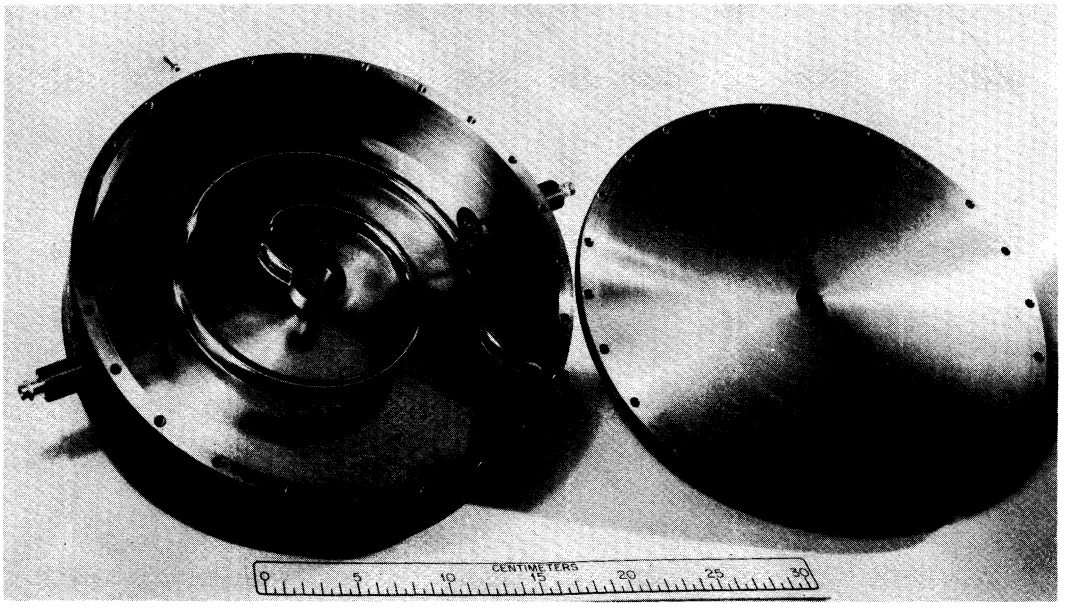

FIGURE 5 A spiral loaded cavity. Illustrated is cavity No. 11 of Table I.

from electric field measurements† and use of (1). The value of L used in (1) was the axial length over which the field was nonzero; this length was always slightly greater than the physical length on axis (partly due to field fringing into (beam) end ports and partly due to bead finite diameter which was 0.7 cm in most measurements).

The normalized shunt impedances of Table I are plotted in Figure 2. Although points do not fall exactly on the theoretical curve we feel that the data confirm the basic results of the model because of two observations. First, the form of the theoretical curve and that of a smooth-fit curve to the data are nearly the same. Second, as Δ/d_0 becomes larger the results approach the theoretical curve as expected from the derivation which assumed Δ/d_0 large.

It is interesting to note from Figure 2 that the data approach the theoretical curve from the low side. Since it is known that some cavities also with $1 \leq \Delta/d_0 \leq 3$, measure above the curve (as discussed in the next section), we conclude that neither L or Δ seem to hold the main key to designing very high values of normalized shunt impedance in spiral cavities.

In the process of measuring shunt impedance, axial electric field distribution was measured for each cavity. Figures 6 and 7 illustrate results for cavities where $\Delta/d_0 = 1.0$ and $\Delta/d_0 = 3.0$ respectively. Results for the intermediate cavity ($\Delta/d_0 = 2.0$) were quite similar to those of Figure 7. The results were highly symmetric about the cavity center, so only half of the total plot is illustrated.

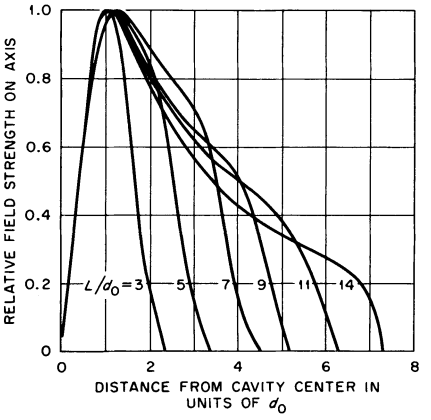

FIGURE 6 Relative electric field strength on axis for cavities with spiral gap spacing Δ of one tubing diameter d_0.

Using the measured electric field distributions with Eq. (3) values of ρ^2 were obtained by numerical integration. These are given in Table I. By application of Eq. (2) effective shunt impedance is easily found. Cavity 5 has the highest value of Z_{eff} (26.94 MΩ/m). However, cavity 16 is actually the

† Obtained by Slater's perturbation method using a dielectric bead.

TABLE I

Measured parameters for 17 copper cavities having spirals with circular cross section

Cavity No.	L (cm)	$\frac{\Delta}{d_0}$	f_0 (MHz)	Q_0	Z (MΩ/m)	$\frac{R_s l \varepsilon_r Z}{3600\,\pi^3}$	ρ^2
1	17.78	1	172.24	3211.6	25.18	0.402	0.444
2	13.97	1	170.49	3263.6	31.94	0.507	0.489
3	11.43	1	167.86	3189.0	35.71	0.563	0.519
4	8.89	1	161.16	3071.4	40.22	0.625	0.572
5	6.35	1	155.64	2786.5	43.80	0.664	0.615
6	3.81	1	144.93	1970.8	31.42	0.405	0.647
7	17.78	2	119.10	3775.0	33.88	0.630	0.458
8	13.97	2	116.37	3558.9	39.84	0.731	0.496
9	11.43	2	113.17	3553.0	43.43	0.786	0.533
10	8.89	2	109.63	3196.0	43.20	0.770	0.572
11	6.35	2	105.29	2621.8	36.77	0.642	0.612
12	3.81	2	101.25	1667.0	19.94	0.342	—
13	17.78	3	90.92	3928.0	38.42	0.788	0.448
14	13.97	3	88.54	3670.3	41.55	0.841	0.482
15	11.43	3	86.50	3479.9	43.37	0.868	0.519
16	8.89	3	84.12	3276.0	43.78	0.864	0.554
17	6.35	3	81.84	2649.2	37.06	0.721	0.608

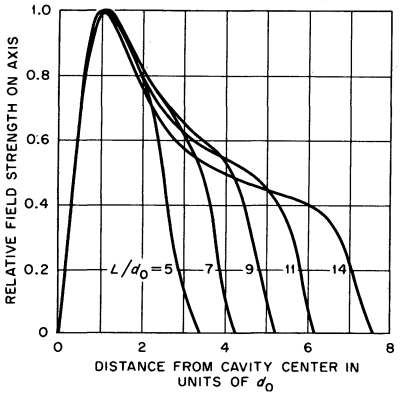

FIGURE 7 Relative electric field strength on axis for cavities with spiral gap spacing Δ of three tubing diameters d_0.

best cavity ($Z_{\text{eff}} = 24.25$ MΩ/m) because the normalized effective shunt impedance is largest† ($R_s l \varepsilon_r Z_{\text{eff}}/3600\pi^3 = 0.479$).

As a function of L/d_0 we find that ρ^2 is nearly independent of relative spiral gap spacing Δ/d_0. Thus, on the basis of these data, if one seeks to maximize Z_{eff} by choice of ρ^2, gap spacing has little effect. On the other hand, since ρ^2 increases as L/d_0 decreases, we see that the optimum ratio L/d_0 for maximizing normalized Z_{eff} is slightly smaller than the optimum ratio for maximizing normalized Z.

OTHER EXPERIMENTAL DATA

Bendt, Erkkila, and Stokes[2] have given data on 27 copper SLC's, of which 23 use single spirals with circular cross section. Shunt impedance of the 23 units has been normalized using the relationship $R_s c \varepsilon_r Z/14{,}400\pi^3 f$ and plotted on Figure 8 which also reproduces the theoretical curve for comparison. Cavities of Ref. 2 are identified by frequency in Table II. The amount that a given cavity result deviates from the theoretical curve (as a percentage) is also given in Table II. Thus, cavity number 20 may be considered the best cavity since it is 44.5% above the curve while cavity 18 is the worst at 46.2% below the curve.

There are primarily nine parameters‡ affecting the design of a SLC. They are: frequency, shell length L, shell diameter D, tubing diameter d_0, spiral air gap spacing Δ, number N of spiral turns, stem length A, drift tube length L_D and drift tube diameter D_D. All of these are physical parameters

† Scaling cavity 16 to the frequency of cavity 5, we expect $Z_{\text{eff}} = 32.99$ MΩ/m to be achievable for the best cavity.

‡ There are clearly others such as shape and thickness of the drift tube, tubing cross-sectional shape of the spiral, etc. These may for the present analysis be considered constant.

TABLE II

Parameters applicable to 23 cavities from Ref. 2

Cavity no.	Frequency f (MHz)	Shunt impedance Z (MΩ/m)	Deviation of Z from curve (%)	D/d_0	Δ/d_0	A/d_0	L_D/d_0	D_D/d_0
1	44.41	28.6	−17.5	41.01	2.53	5.06	3.22	4.81
2	51.14	42.5	15.0	34.11	2.11	4.22	2.67	4.00
3	46.65	39.6	21.1	25.51	2.36	2.76	5.00	2.99
4	48.92	38.9	7.1	41.01	3.16	5.06	12.91	4.81
5	80.45	31.9	−34.0	26.53	—	—	3.16	4.00
6	83.15	38.5	−18.4	26.53	—	—	4.82	4.00
7	84.29	35.7	−21.6	26.53	—	—	6.48	4.00
8	86.81	31.4	−28.8	26.53	2.11	3.68	7.14	4.00
9	81.09	26.5	−40.7	26.53	2.63	4.22	10.69	4.00
10	84.35	24.5	−38.4	26.53	—	—	10.51	4.00
11	93.70	29.4	−41.2	26.74	2.63	3.16	3.16	2.67
12	93.80	38.1	−19.0	26.53	3.16	6.84	3.16	4.00
13	106.16	40.9	−13.3	41.01	1.27	8.86	3.67	4.81
14	111.38	40.6	−15.9	41.01	2.53	7.59	3.67	4.81
15	99.23	36.8	−23.9	26.53	3.16	6.84	5.37	4.00
16	99.48	34.8	−28.2	26.53	3.16	6.84	6.32	4.00
17	104.90	31.8	−40.0	26.74	3.16	4.22	7.16	4.00
18	96.86	28.8	−46.2	20.00	—	—	8.03	2.99
19	101.29	27.9	−44.1	32.15	3.80	3.48	12.91	4.81
20	99.47	74.6	44.5	31.25	2.60	2.60	3.13	2.25
21	99.85	59.5	15.0	31.25	2.60	2.60	3.13	3.67
22	99.69	63.5	32.0	50.63	1.56	11.72	2.34	2.34
23	101.29	59.6	31.2	52.92	2.60	13.54	3.13	3.67

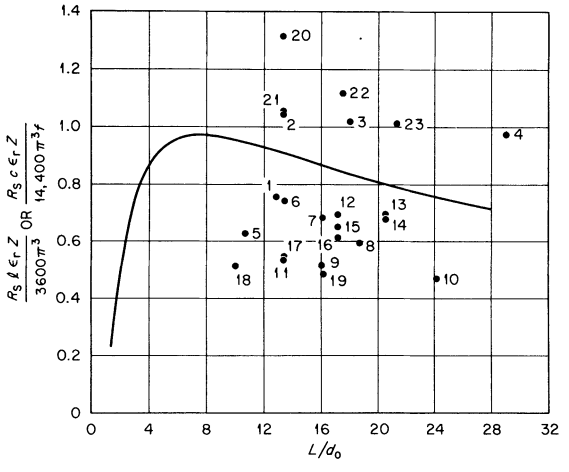

FIGURE 8 Normalized, measured bare shunt impedance values for 23 spiral loaded cavities at taken from the literature. Also shown for comparison is the theoretical curve reproduced from Figure 2.

except for frequency which may be eliminated from consideration by scaling all physical dimensions suitably. Furthermore, if we accept the general behavior of shunt impedance as a function of L as not being too different than predicted by the theoretical curve, L may be eliminated from consideration. Next, if we observe from Ref. 2 that both good and poor cavities may be obtained for most of the spiral turn numbers used, we may omit N from further consideration. Finally, if we eliminate d_0 by normalizing the remaining parameters we need consider only D/d_0, Δ/d_0, A/d_0, L_D/d_0, and D_D/d_0. Using available values for Δ and A (Ref. 4) these quantities are listed in Table II. Using the normalized parameters, comparisons were made of good versus poor cavities using three criteria. First is the relative position of the span of the parameters (minimum to maximum range), second, the parameter averages, and third the best/worst parameter values. While no really consistent pattern could be found in the data, we were able to observe the direction of parameter choices in design.

All three criteria seemed to support the fact that normalized shell diameter D/d_0 should be large. Two criteria seem to weakly indicate that normalized gap spacing Δ/d_0 should be small while normalized stem length A/d_0 should be large (no data were available for Δ or A for the worst cavity

so best/worst cavities could not be compared). All three criteria also seemed to indicate that normalized drift tube length L_D/d_0 and diameter D_D/d_0 should be small for higher shunt impedance.

We recognize that "large" and "small" have no absolute meaning. They are used here only to imply the values of some parameters of the better cavities in relation to those of the poor cavities. On the other hand, examination of the data does seem to imply that, if a nominal set of parameters were to be chosen about which a systematic set of measurements was made to find the near-optimum parameters, a reasonable choice would be $D/d_0 = 35$, $\Delta/d_0 = 2$, $A/d_0 = 7$, $L_D/d_0 = 3$, and D_D/d_0 2.2.

CONCLUSIONS

Using a quarter-wavelength shorted transmission line as a model for a loosely wound SLC having a large shell diameter, bare shunt impedance has been found as plotted in Figure 2 for spirals with circular cross section. Figure 3 is the similar result for rectangular cross sections. The circular cross section produces the higher bare shunt impedance. New measurement data on 17 cavities were described which gave support to the validity of the theoretical bare shunt impedance curve for spirals with circular cross section. Some data were also included on the distribution of electric field magnitude along the cavity axis and on effective shunt impedance.

By considering measured data from reference 2 it was shown that the theoretical curve forms a good dividing line for classifying "good" and "poor" SLC's. Analysis of the two classes of measured data seems to indicate that cavities with better shunt impedance tend to have large shell diameter, small spiral air gap spacing, large stem length, small drift tube length, and small drift tube diameter. Although "small" and "large" tend to have little absolute meaning the authors feel that indicated values of $D = 35d_0$, $\Delta = 2d_0$, $A = 7d_0$, $L_D = 3d_0$, and $D_D = 2.2d_0$ would be an appropriate set of nominal parameters about which a set of systematic measurements could be made to seek a near-optimum parameter set.

ACKNOWLEDGEMENTS

The authors express their appreciation to Dr. R. H. Stokes for providing them with pre-publication data measured at Los Alamos Scientific Laboratory.

REFERENCES

1. G. J. Dick and K. W. Shepard, A spiral loaded low-β accelerating structure, *Applied Physics Letters*, **24**, 40 (1974).
2. P. J. Bendt, B. H. Erkkila, and R. H. Stokes, Los Alamos Report LA-UR-74-211, 1974, unpublished.
3. G. Dôme, Chapter Cl. le of *Linear Accelerators*, edited by P. M. Lapostolle and A. L. Septier (North-Holland Publishing Co., Amsterdam, 1970), pp. 637 and 653.
4. R. H. Stokes, private communication.
5. International Telephone and Telegraph Co., *Reference Data For Radio Engineers*, Howard W. Sams & Co., Inc., 1969, p. 22–23.
6. H. A. Wheeler, Formulas for the skin effect, *Proc. I.R.E.*, vol. 30, Sept. 1942, pp. 412–424, Eq. 18.
7. S. B. Cohn, Problems in strip transmission lines, *I.R.E. Trans. on Microwave Theory and Techniques*, **MTT-3**, No. 2, 119 (1955).